Supplementary Information

Ionic Intercalation in Two-Dimensional Van der Waals Materials: *In Situ* Characterization and Electrochemical Control of the Anisotropic Thermal Conductivity of Black Phosphorus

Joon Sang Kang, Ming Ke, Yongjie Hu*

Department of Mechanical and Aerospace Engineering

University of California, Los Angeles

Los Angeles, California 90095, United States

*Corresponding author. Email: yhu@seas.ucla.edu

Materials and Methods

Fabrication of electrochemical BP device for *in situ* thermal measurement.

The electrochemical device (representing a battery structure) was fabricated in an Argon-rich glovebox. The detailed fabrication steps for *in situ* measurement are presented in Figure S1. A millimeter-sized glass window was fabricated onto a battery case to provide optical transparency for the TDTR measurement. The window was closed with quartz and completed sealed with chemically inert epoxy. A copper film was used as current collector for the Al-coated BP electrode. All exposing to the electrolyte were blocked off by applying a layer of epoxy to prevent degradation. Electrolyte (1M $LiPF_6$ in 1:1 w/w ethylene carbonate/diethyl carbonate from Sigma Aldrich), separator (Celgard separator), and anode (lithium pellet) were stacked over the BP. The whole battery cell was closed and airtight sealed with epoxy to maintain the chemical stability. The sealing condition was tested to ensure the batteries function properly after several months after fabrication without chemical degradation.

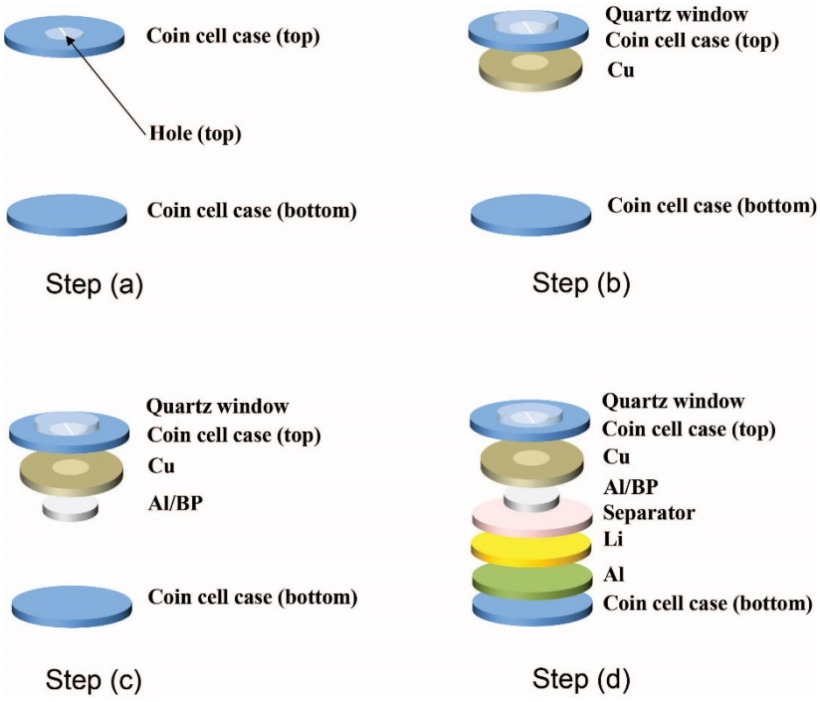

Figure S1. Schematics and device fabrication sequence for *in situ electrochemical and optical-*

thermal measurement.

Raman spectroscopy. The Raman microscope (Renishaw) is using 633 nm wavelength of the laser, with 50× objective lens and power less than 1 mW. The grating resolution of the Raman microscope is 1800 gr/mm.

Electrochemical measurement. The electrochemical measurements and ionic intercalation control were performed using a BioLogic VSP-300 electrochemical station. The galvanostatic discharge was done with a constant current smaller than 3.0 μA and the control of the battery potential from 2.1 V to 0.01 V. The ionic intercalation discharge process was done by decreasing the voltage of a fully charged BP battery with a step size smaller than 0.05 V. For each step, before the thermal measurement, the battery device was held at the constant voltage for more than 3 hours until battery current reduces to a small level (< 10 pA), to ensure that Li intercalation is complete and Li_xP reaches a stable status. The reversibility cycling of a BP battery was done in the reversible voltage range between 2.0 V and 0.78 V using constant currents of 1 μA for charging and discharging, respectively.

TDTR technique for cross-plan thermal conductivity measurement. Ti:Sapphire oscillator (Tsunami, Spectra-physics) generates 800 nm wavelength, femto-second pulse width, and 80 MHz repetition rate beam. Astigmatic and elliptic beam was corrected by a pair of cylindrical lenses and spherical lenses. The beam was divided into pump and probe beam by polarizing beam splitter with large ratio. The pump beam was sinusoidally modulated by passing through the electro-optic modulator (EOM) up to 20 MHz and fundamental frequency of pump beam was doubled by bismuth triborate crystal (BIBO). Probe beam was delayed using mechanical delay

stage from 0 to 6 ns. The probe beam measured the reflectance change introduced by the pump beam. We used concentric and relatively large beam spot size for cross-plan κ measurement (Pump: 50μm, Probe: 10μm ($1/e^2$ diameter)). The reflectance signal was measured and recorded by lock-in amplifier connected with EOM, providing in-phase signal (V_{in}) and out-phase signal (V_{out}). The amplitude, $\sqrt{V_{in}^2 + V_{out}^2}$, and phase signal, $\tan^{-1}(-\frac{V_{out}}{V_{in}})$, were used to compare with thermal model for extracting thermal properties. For fitting anisotropic materials, the anisotropic ratio of an in-plane thermal conductivity to cross-plane conductivity was included in the thermal model. The cross-plane analysis was performed iteratively with the in-plane analysis.[1]

BO-TDTR technique for in-plan thermal conductivity measurement. The in-plan thermal conductivity (κ_{ZZ} and κ_{AC}) were measured at fixed delay time (-50 ps) and 1.5 MHz modulation frequency. We used small beam radius (1.85 μm) for in-plan measurement with ×50 objective lens. The beam diameter was measured with both knife-edge beam profiler (BP-209VIS) and TDTR signal at short positive probe delay time (+50 ps) with high modulation frequency (9.5MHz). Pump beam was swept by motorized piezo-mirror mount (Newport model 8809) with 0.7 μrad of step resolution, or corresponding to a spatial resolution down to 2 nm on the sample surface. During measurement, we double checked laser conditions, including spot size, beam alignment offset and power, and made sure these parameters are not changing along the delay stage. The V_{out} signal was recorded by lock-in amplifier and thermal model fitting is performed to extract the FWHM of V_{out} signal. The FWHM was converted to in-plane κ by thermal conductivity tensor model[1]. For in-plane fitting, the cross-plane thermal conductivity and interface conductance was included in the thermal model. The in-plane analysis was performed iteratively with the cross-plane analysis.

Thermal conductivity modeling. The reflectance signal of linear time invariant system detected by RF lock-in amplifier is expressed by

$$Z(f_0) = \sum_{N=-\infty}^{\infty} H(f_0 + Nf_s)\exp(iNf_s\tau) \quad [1]$$

where f_0, f_s, N, and τ are the modulation frequency, probe frequency, integer, and delay time. The in-phase signal (V_{in}=Re[Z(f_0)]) is related with temperature response from sample surface and the out-of-phase signal (V_{out}=Im[Z(f_0)]) is from the imaginary temperature oscillation[2]. The frequency domain solution to temperature fluctuation in TDTR (both conventional and beam offset TDTR) is expressed by[1,3]

$$H(f) = \frac{2\pi}{A_0}\int_0^{\infty} B(f,k)P(k)S(k)kdk \quad [2]$$

where B is the temperature fluctuation contributed by thermal properties of sample obtained from multi-layer thermal modeling.[3] P and S are the Gaussian beam intensity profile of pump and probe beam respectively. In different with conventional TDTR, the S in the beam offset TDTR is expressed by[4]

$$s(x,y) = \frac{2A_0}{\pi w_s^{\,2}}\exp\left(-\frac{2((x-x_0)^2+y^2)}{w_s^{\,2}}\right) \quad [3]$$

where A_0, w_s, and x_0 are the total laser intensity, probe beam spot size, and offset between pump and probe beam. Detailed step for Hankel transform from *s(x,y)* to *S(k)* is shown in Ref.4. When the pump beam spot size is comparable or smaller than the in-plane thermal diffusion length, beam offset in lateral direction contains in-plane thermal properties of sample and V_{out} become proportional to the exp ($-x_0^2/L_p^2$).[1] By extracting full width half maximum (FWHM ~ κ), in-plan thermal conductivity can be obtained along with beam offset direction.

***In situ* thermal characterization integrating TDTR and electrochemical measurement.** The BP battery was aligned with crystal orientation on the rotational sample holder and combined with both TDTR and electrochemical station for *in situ* thermal properties measurements. The pump and probe spot was set to a fixed position on the sample surface to minimize measurement error from the non-uniformity of Al thickness and variations in the laser focal plan. We used a voltage step smaller than 0.1 V to control the Li concentration. After each voltage step decrease, we allowed sufficient time (more than 3 hours) for the lithium interaction process to ensure complete lithium intercalation and an equilibrium state of the Li_xP. We set the voltage range from 2.0 V to 0.78 V for the reversible regime measurement and use voltage smaller than 0.01 V for the irreversible stage (Li_3P). The process was monitored and verified by the current measurement using the electrochemical station. TDTR measurement was performed after the current is negligible and the battery reaches a steady charge state.

References

(1) Feser, J. P.; Liu, J.; Cahill, D. G. *Rev. Sci. Instrum.* **2014**, *85* (10).

(2) Liu, J.; Choi, G. M.; Cahill, D. G. *J. Appl. Phys.* **2014**, *116* (23).

(3) Schmidt, A. J.; Chen, X.; Chen, G. *Rev. Sci. Instrum.* **2008**, *79* (11).

(4) Feser, J. P.; Cahill, D. G. *Rev. Sci. Instrum.* **2012**, *83* (10).